2018 IEEE/RSJ International Conference on Intelligent Robots and Systems (IROS)
Madrid, Spain, October 1-5, 2018

# Modeling and Control of an Articulated Tail for Maneuvering a Reduced Degree of Freedom Legged Robot

Wael Saab, Jiteng Yang, and Pinhas Ben-Tzvi, *Senior Member, IEEE*

***Abstract*— This paper presents dynamic modeling and control of an articulated robotic tail to maneuver and stabilize a reduced degree-of-freedom (DOF) quadruped robot. Conventional legged robotic systems consist of leg mechanisms that provide simultaneous propulsion, maneuvering and stabilization. However, in nature animals have been observed to utilize their tails to assist the legs in multiple tasks. Similarly, by incorporating an articulated tail onboard a quadruped robot, dynamic tail motions can be used to aid maneuvering. Therefore, tail implementation can potentially lead to simplifications in design and control of the legged robot since the legs will be responsible for only propulsion tasks. In this paper, a robotic system design consisting of an articulated tail and quadruped robot system is presented. Dynamic models are derived to analyze an optimal tail mass and length ratio to enhance inertial adjustment applications and develop an outer loop controller to plan tail trajectories for desired maneuvering applications. Results of analytical optimization are corroborated with measured data from biological animals. To decouple the dynamics of the articulated tail mechanism an inner loop controller using feedback linearization maps the desired behavior to the actuator inputs. This approach is validated using hardware-in-the-loop experiments with tail prototype in conjunction with simulated quadruped platform. Results demonstrate the capabilities of the articulated tail in enabling precise left and right turning (maneuvering).**

## I. Introduction

In nature, animals use their tails to assist different locomotive functions. In terms of maneuvering, cheetahs utilize high-speed tail motions to maintain body roll while chasing pray [1]. Similarly geckos and the green anole lizards use their tails to reorient their bodies in midair to prevent injury during landing [2, 3]. In term of stabilization, cats and the wall lizard use their tails as an active counterbalance to enhance their mass distribution [4, 5]. Hence, a tail can be used as a method to initially adjust the body using either static or dynamic motions without interacting with the environment. This feature is beneficial for the robot in an environment where ground contact cannot be guaranteed.

To this date, the majority of research on bioinspired or biomimetic legged robots has focused on using leg mechanisms for simultaneous propulsion, and maneuvering (left and right turning) [6]. Conventional quadruped robots require a minimum of 3 active degrees of freedom (DOF) for each leg. Therefore, the robot must simultaneously control a minimum of 12 active DOFs using sophisticated algorithms with articulated leg designs.

This research aims at utilizing an articulated tail to reduce the required burden on the legged robot for maneuvering tasks. Figure 1 shows the tail-quadruped system under study. The system is composed of a quadruped robot, constructed with four Robotic Modular Legs (RML) [6] and the Roll-Revolute-Revolute Robotic Tail (R3-RT) [7]. RMLeg is a 2 DOF planar mechanism to drive the robot moving forward and tail is used for steering (maneuvering).

This paper is presented as follows: Section II reviews prior work on robotic tails and control of hyperredundent robots. Section III describes the robotic system. Section IV and V extends the authors previous work that analyzed pendulum-like tail implementation [7] to develop kinematic and dynamic models of a legged robotic system with an attached articulated tail that are used to select optimal tail mass and length ratios to maximize inertial adjustment applications with comparative analysis to biological animal data. Based on these dynamic formulations, Section VI defines the outer and inner loop control laws to plan tail trajectories and decouple articulated tail dynamics for trajectory tracking that of goal oriented maneuvering behavior. Section VII presents the hardware-in-the-loop experiments to validate the control laws using the articulated tail prototype in conjunction with a virtual quadruped robot. Section VIII concludes the paper and presents the future works.

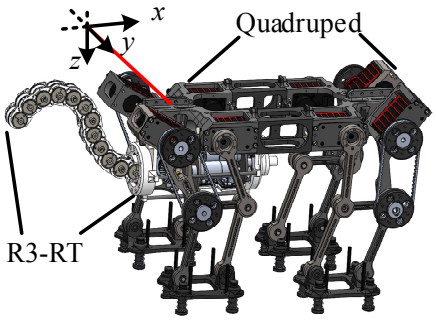


Fig.1 Legged robotic system: Quadruped with an attached R3-RT.

## II. Background and Motivation

This section presents an overview of previous work in the field of robotic tails and hyperredundent manipulator control.

### A. Robotic Tails

Robotic tail implementation onboard mobile robots has focused on rigid-body pendulums that either rotate about a single pitch/roll/yaw DOF or are capable of spatial motion using combined pitch-yaw, yaw-pitch, or roll-pitch DOFs

*This material is based on work supported by the National Science Foundation under Grant No. 1557312

W. Saab, J. Yang, and P. Ben-Tzvi are with the Robotics and Mechatronics Lab, Virginia Tech, Blacksburg, VA 24060 USA (email: {waelsaab, yjt, bentzvi}@vt.edu)

about the tail base [8]. Such pendulum-like tails have been used for: 1) propulsion to actuate walking [9], and enable rapid acceleration or deceleration of the robot [10], 2) maneuvering to aid steering [11] and airborne pitch adjustment [12], and 3) stabilization to aid disturbance rejection [1], and balancing [13].

Recent research has investigated the benefits of articulated robotic tails. In work presented by Rone and Ben-Tzvi [14], simulation results indicate that tail articulation can enhance inertial loading, used to maneuver a quadruped robot, in comparison to a pendulum-like tails performing a similar motion due to additive velocities and accelerations along the articulated tail joints. These results were corroborated by comparing experimentally measured results of inertial loading profiles of an articulated tail with its pendulum-like counter counterpart [15]. Results indicated that tail articulation increases inertial moments about the base by 53 % which is useful for inertial adjustment applications and decreases generated inertial forces by a net factor of 44% that cause undesirable translation of the robotic system it is attached to. This research aims to continue in the direction of implementing an articulated serpentine-like tail onboard legged robot to formulate dynamic models used for optimization and control for inertial adjustment applications.

### B. Hyperredundent Robot Control

The proposed articulated serpentine-like robotic tail to be used onboard the quadruped robot is a hyperredundent manipulator since it is composed of significantly more joints than task space coordinates. Prior research into controllers that do not include system dynamics include PID and PD based approaches for individual joint actuation [16] or segment curvature tracking of continuously deforming manipulators [17]. Another approach to controlling hyperredundent manipulators includes, neural network based controllers that use online tuning of network parameters during operation as either a standalone controller [18] or as a feedforward contribution that employs a non-model-based nonlinear feedback loop [19]. Model based control approaches, such as the Jacobian method maps task space sensor data into joint space [20-22] or dynamics based models [23] augment aspects of non-model based approaches for more accurate performance of hyperredundent robot control.

## III. Robotic System

Figure 1 shows isometric views of the robotic system consideration that consists of a quadruped robot with an attached R3-RT [15]. The quadruped robot is composed of four Robotic Modular Legs (RML) [24, 25] capable of performing planar walking gaits that enable planar forward locomotion. It is envisioned that dynamic motions of the articulated tail will enable enhanced maneuvering capabilities without the requirement of ground contact. It is assumed that during a walking gait the legs do not significantly change the mass properties of the robot. The tail is composed of an actuation unit that houses a geared motor assembly and articulated tail segments that are driven via cable transmission systems.

### A. Quadruped Robot

Figure 2(a) shows a schematic representation of the quadruped robot. Each RML is a two-DOF planar mechanism composed of two serially connected four-bar mechanisms. The two four-bar mechanisms have parallelogram topologies, which result in double-rocker behavior. This guarantees a parallel flat foot orientation with respect to the quadruped body without needing an additional actuator between the shin and foot links. On flat surfaces, flat feet provide a more stable support polygon compared to feet with a point or line contact.

The quadruped is designed to provide forward locomotion along a single direction, with the tail capable of performing the maneuvering functions. A trot gait pattern is utilized in which the legs alternate between a straight line support phase with constant velocity, in which the foot is in contact with the ground, and a swing phase, in which it is airborne.

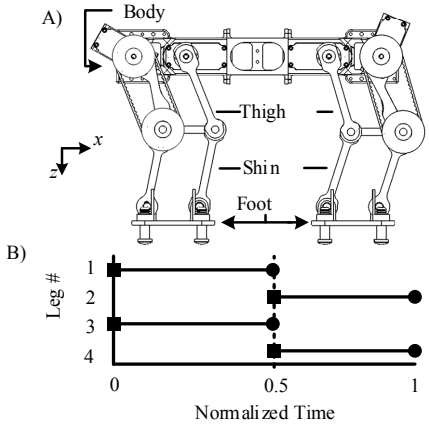


Fig. 2 A) Legged robot schematic representation, B) quadruped gait diagram.

Figure 2(B) illustrates the gait diagrams used for sequencing the quadruped legs for a trot gait. The plot's horizontal axis spans the normalized time for a single foot trajectory cycle. The line segment for each leg represents the support phase, from landing (square at start) to takeoff (circle at end). Trot gaits provide quadrupeds with planar foot contact a quasi-statically stable walking gait if the quadruped's zero-moment point falls within the support polygon created by the geometric boundary created by all of the ground contact points at a given time. The quadruped alternates between diagonal pairs of legs in contact with the ground. Therefore, two support phase feet move cooperatively (i.e., in the same direction) for forward walking and the system zero-moment point can be configured such that it always falls within the support polygon.

### B. Tail Subsystem

Figure 3 shows the R3-RT used as the tail subsystem on the quadruped robot for this analysis. The R3-RT consists of a rigid housing, an actuation module, and one articulated manipulator composed of two independently actuated tail segments. The rigid housing connects to the quadruped subsystem and provides support for two coaxial bearings in which the actuation module is mounted. The actuation module contains the three motors used to actuate the R3-RT.

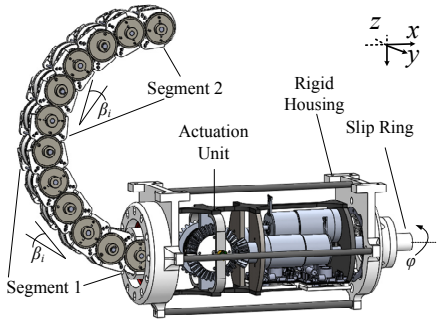


Fig. 3 R3-RT subsystem design.

The articulated tail structure consists of 2 independently actuated segments each consisting of 6 links serially connected to one another and the actuation module through parallel joints. Two actuated segments are created by two pairs of cables that route along the links: the first segment is created by terminating one cable pair at link 6, while the other cable pair terminates at link 12. Five equal-pitch gear pairs within each segment ensure the six relative joint angles $\beta_i$ in that are equal, and cable routing along nested cylindrical surfaces ensures that cable displacements are equal and opposite, allowing a single spool to drive each cable pair. The segments' actuation is decoupled by utilizing an S-curve cable routing for the segment 2 cabling through segment 1. In this paper, the segments are synchronized to rotate along the same direction; therefore creating C-shaped tail configurations as shown in Fig. 3. Additional details on the design and analysis of the R3RT can be found in [15,26].

## IV. Kinematic Analysis

This section presents kinematic analysis of the robotic system, to derive the relations that will be used to develop the dynamic relations derived in the next section.

Figure 4 shows free body diagram of a generic legged robot with an attached *n*-link articulated tail. A body attached frame (O′, $\mathbf{b}_1$, $\mathbf{b}_2$) is fixed to the legged robot at $O'$ = ($x_0$, $y_0$). The bodies are modeled as point masses $m_0$ (tail actuation unit), $m_1$ (legged robot body), and $m_{2\text{-n}}$ (tail linkage mass). The indices $i$ = {0, 1, 2-n} refer to the tail actuation unit, legged robot, and tail linkages, respectively. In the figure, the legged robot and tail are disconnected at the tail revolute joint. $m_0$ is located at point $O'$. The legged robot and tail can rotate relative to one another, about the $\mathbf{e}_3$-axis. The yaw angle of the legged robot and relative angle of the tail input pulley rotation for segment 1 and 2 are defined as $\theta$ , $\beta_{seg,1}$, and $\beta_{seg,2}$, respectively. We define the relative link rotations to be $\beta_{1\text{-}n}$.

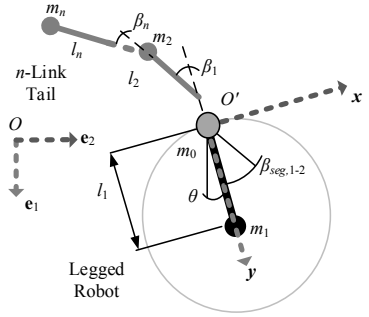


Fig. 4 Schematic diagram of a robotic system consisting of a lumped parameter legged robot and an *n*-link articulated tail.

Here, $m_i$ represents lumped masses, $\boldsymbol{v}_i$ is the mass velocity, $\boldsymbol{R}_i$ is the position vector locating the masses relative to $O'$, and $l_i$ represents a length of body $i$ or effective length of the robot.

The relation of joint angles are defined as

$$\beta_i = \begin{cases} \eta_i\beta_{seg,1}, i=1 \quad \eta_i\beta_{seg,1} - \sum_{j=1}^{i-1}\beta_j, 1<i\le 6 \\ \eta_i\beta_{seg,2}, i=7 \quad \eta_i\beta_{seg,2} - \sum_{j=1}^{i-1}\beta_j, 7<i\le 12 \end{cases} \tag{1}$$

where $\eta_i$ represents the coupling ratio of the $i$-th tail joint angle with respect to the input pulley rotation. Since the R3-RT tail is constrained with gears of equal pitch diameter and each segment has six links; therefore, $\eta_i$ = 1/6. With reference to Fig. 4, the COM location and the total angular momentum of the system are defined to be

$$\begin{bmatrix} \boldsymbol{x}_c \\ \boldsymbol{y}_c \end{bmatrix} = \sum_{i=0}^{n} \frac{\boldsymbol{R}_i m_i}{m_i} \tag{2}$$

$$\boldsymbol{H}_O = \sum_{i=0}^{n} m_i \boldsymbol{R}_i \times \dot{\boldsymbol{R}}_i \tag{3}$$

## V. Dynamic Analysis

Multi-segment models that conserve angular moment during air born phases have been presented for describing the motion of a falling cat [5], geckos jumping between planes of various angular orientation [3], humans in space [27], and active-hinged cellular phones [28]. In this analysis we utilize the assumption of conservation of angular momentum to develop the dynamic formulations describing the angular variation of a legged robot due to high-speed articulated tail motions.

In earlier studies, it was found that the friction at the feet during a quasi-static walking gait limited effective turning using high-speed tail motions[7]. This challenge could be mitigated by choosing to actuate the tail during an airborne gait phase in which all legs are lifted from the ground. A small hop is applied during the walking trajectory to lift the legged robot off the ground for 0.45 seconds and actuate the tail during this time for maneuvering. It is assumed that during tail motions for maneuvering applications, angular momentum will be conserved, therefore, $\boldsymbol{H}_0 = \mathbf{0}$, and $\mathbf{x}_c$ and $\mathbf{y}_c$ are constants of motion [7].

Using this reasoning, taking the time derivative of Eq. (2) and substituting it into Eq. (3) knowing that $\dot{\boldsymbol{x}}_c = \dot{\boldsymbol{y}}_c = \mathbf{0}$ yields the relation for the velocity of the actuation unit given by

$$\dot{\boldsymbol{R}}_0 = \begin{bmatrix} \dot{\boldsymbol{x}}_0 \\ \dot{\boldsymbol{y}}_0 \end{bmatrix} = f(m_i, l_i, \theta, \dot{\theta}, \beta_{seg,1\text{–}2}, \dot{\beta}_{seg,1\text{–}2}) \tag{4}$$

Substituting Eq. (4) into Eq.(3), where $\boldsymbol{H}_0 = \mathbf{0}$ due to conservation laws yields an expression for the legged robot angular velocity variation as result of high-speed articulated tail motion

$$\dot{\theta} = -f(m_i, l_i, \beta_{seg,1})\dot{\beta}_{seg,1} - f(m_i, l_i, \beta_{seg,2})\dot{\beta}_{seg,2} \tag{5}$$

Numerical integration of Eq. 5 yields the relation of angle variation defined by

$$\Delta\theta = -\int f(m_i, l_i, \beta_{seg,1})d\beta_{seg,1} - \int f(m_i, l_i, \beta_{seg,2})d\beta_{seg,2} \quad (6)$$

### A. Tail Geometric and Mass Parameter Optimization

Previous approaches of scaling pendulum-like tails have utilized *efficacy* that relates constant inertia of a pendulum to that of the legged robot [29]. This criteria cannot be used for scaling an articulated tail due to varying inertia properties during motion. This section presents analysis to optimize the R3-RT onboard the quadruped robot to maximize angular variation effects due to high-speed tail motions. The mass and length ratio is defined as $\sigma = \sum_{i=2}^{n} m_i / (m_0 + m_1)$ and $\lambda = \sum_{i=2}^{n} l_i / l_1$, respectively.

For the robotic systems under consideration (Fig. 1) consisting of a quadruped robot with a 12–link tail with constant properties $m_1$ = 5.7 kg, $m_0$ = 3.1 kg, and $l_1$ = 0.5 m, Eq. (6) was evaluated to compute $\Delta\theta$ for a prescribed tail motion of $\Delta\beta_{seg,1\text{-}2}$ = 60° while varying σ and λ. Results of this analysis are presented as a contour plot in Fig. 5. The tangency of the contour lines of constant $\Delta\theta$ or observable rate of color change indicates the amount of sensitivity with respect to variations of σ and λ. By first analyzing the effects of varying mass ratio, it is interesting to note that the tangency for the lines of constant $\Delta\theta$ is greatest within the range of $\sigma$ < 0.5. Similarly, by observing the contour plot rate of color change along the vertical axis, the rate of change is greatest for λ < 2. Thus, indicating that angular variation becomes less sensitive with increased mass and length ratios beyond these thresholds.

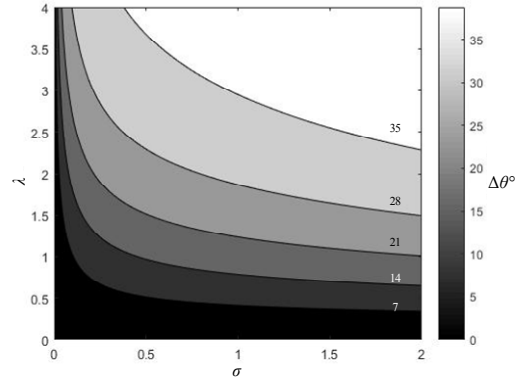


Fig. 5 Angular variation plot for the quadruped and R3-RT system resulting from a $\Delta\beta_{seg,1\text{-}2}$ = 60° tail motion for various mass/length ratio.

### B. Comparison to Biological Tails

This section compares the optimal ranges computed via the angular variation relation as observed from Fig. 5 with measured mass and length ratios of biological animals which range in topology; however, utilize their tails for maneuvering and stabilization applications as described in section I.

Table I presents the mean measured mass and length ratio for animals that utilize their tails for maneuvering and stabilization. It can be noticed that mass and length ratios of these animals fall within high sensitivity ranges from Fig. 5 equivalent to λ < 2 and $\sigma$ < 0.5. Both the green anole lizard [2], and gecko [3] utilize their tails during aerial flight to induce zero angular momentum reorientations in mid-air to prevent the possibility of injury. It is interesting to note that the green anole has a mass ratio that is a factor of 0.5 less than the gecko's; however, its length ratio is approximately twice as large. In comparison to the gecko, the cheetah's tail length ratio closely matches with a value of λ = 0.9; however, its mass ratio is significantly lower. Recent research by Patel et.al [30] indicates that cheetah's long tail fur results in aerodynamic effects where the tail is used like a *rudder* in air to compensate for its low mass ratio and enhance inertial loading resulting from high-speed tail motions. The wall lizard uses its tail for static stabilization applications, similar to a balancing weight, to more evenly distribute weight over flimsy vegetation and as a counterpoise or coil it wraps around branches while climbing [4]. It is interesting to note that since the tail is not used for dynamic high-speed motions, it tail length and mass ratio is relatively longer and heavier than other animals where $\sigma$ = 0.28 and λ = 2.1; however, both are a factor of ~2 larger than that of the Gecko.

Although there does not exist sufficient measured data from biological animals found in nature to conclude an optimal compromise between mass and length ratios for tail-aided inertial adjustment applications. The results of this comparative analysis corroborate the optimal ranges concluded from analysis of the contour plot presented in Fig. 5 that can be used to further aid the process of scaling articulated tails onboard legged robots to maximize angular variation resulting from high speed tail motions.

TABLE I. MEAN MEASURED MASS AND LENGTH RATIO FOR ANIMALS THAT UTILIZE TAILS FOR MANEUVERING AND STABILIZATION.

| Animal | Tail Parameter | |
|---|---|---|
| | σ | λ |
| Green Anole [2] | 0.05 | 1.82 |
| Gecko [3] | 0.10 | 0.92 |
| Cheetah [31] [32] | 0.02 | 0.9 |
| Wall Lizard [4] | 0.28 | 2.1 |

## VI. CONTROL

This section details the outer-loop and inner-loop control laws, illustrated in Fig. 6, used to operate the robotic system. The outer-loop control law plans the desired tail trajectory that implements goal oriented maneuvering behaviors and the inner-loop control law calculates the desired input angular rotation to be tracked by the articulated tail.

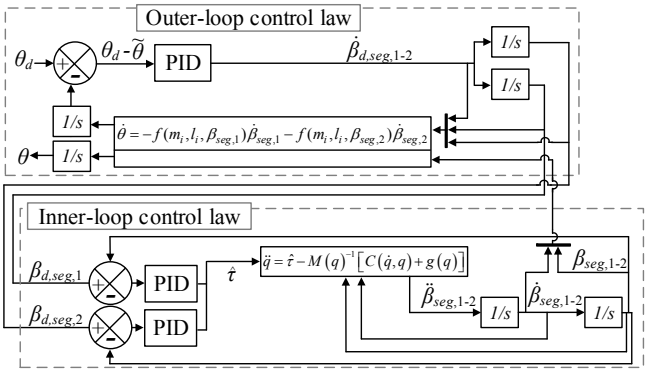


Fig. 6 Tailed quadruped outer- and inner-loop control concept

The set point of the outer-loop controller, Fig. 6, is a desired legged robot orientation $\theta_d$ that represents a desired yaw turning angle for maneuvering. For maneuvering, the tail will produce a planar motion with a fixed roll angle to orient the articulated tail in the ***xy*** plane, a PID comparator outputs a desired tail input velocity $\dot{\beta}_{d,seg,1\text{–}2}$ that is used to synchronize the two tail segments based on feedback from an estimated quadruped angle $\tilde{\theta}$ by integrating the output of the legged robot angular velocity variation Eq. (5). The synchronized angular velocities are integrated to obtain a desired tail trajectory $\beta_{d,seg,1\text{-}2}$ that is fed to the inner-loop control law which is used to control the tail motion to achieve the desired goal orientated behavior.

The controlled tail state variables are defined as $q = [\beta_{seg,1}, \beta_{seg,2}]$. To develop a state based inner-loop controller, the tail dynamic model, previously derived in [15], can be represented as

$$\boldsymbol{M}(\boldsymbol{q})\ddot{\boldsymbol{q}} + \boldsymbol{C}(\dot{\boldsymbol{q}},\boldsymbol{q}) + \boldsymbol{g}(\boldsymbol{q}) = \boldsymbol{\tau} \tag{7}$$

Where $\boldsymbol{M}(\boldsymbol{q})$ is the inertia, $\boldsymbol{C}(\dot{\boldsymbol{q}},\boldsymbol{q})$ is the tail's centripetal and Coriolis effect, $\boldsymbol{g}(\boldsymbol{q})$ is the gravitational effect, and $\tau$ is the input torque. However, to implement a PID based controller for tail trajectory tracking, the dynamic model is decoupled using a nonphysical torque input, $\hat{\tau}$ , as follows

$$\ddot{\boldsymbol{q}} = \hat{\boldsymbol{\tau}} - \boldsymbol{M}(\boldsymbol{q})^{-1}\left[\boldsymbol{C}(\dot{\boldsymbol{q}},\boldsymbol{q}) + \boldsymbol{g}(\boldsymbol{q})\right] \quad \text{where } \hat{\boldsymbol{\tau}} = \boldsymbol{M}(\boldsymbol{q})^{-1}\boldsymbol{\tau} \tag{8}$$

Using this approach, a PID comparator for each segment is used to convert the tail input trajectory errors into $\hat{\boldsymbol{\tau}}$ that is fed into the decoupled dynamic model, Eq. (8), to obtain the tail input angular acceleration as seen in Fig. 6. Integration yields tail angular velocity and orientation that is fed back into the decoupled dynamic model and angular velocity relation for a more accurate calculation of $\theta$. The tail segment angular velocities are sent to motor drivers that regulate motor current as evaluated in [15] to generate accurate dynamic tail motions.

## VII. Simulation and Experimental Results

This section utilizes the R3-RT prototype in conjunction with a quadruped simulation in hardware-in the loop (HIL) experiments (section VII.A) to demonstrate various maneuvering (section VII.B) case studies to validate the control approach defined in section VI with comparison to simulation results.

### A. Experimental Setup

HIL experiments use real, physical system hardware to replace one or more simulated subsystem in an analysis. A prototype R3-RT is used in conjunction with a simulated quadruped walking in a virtual environment on flat terrain using a multi-body dynamics physics simulator MSC-ADAMS, which is capable of solving for the kinematics and dynamics in the presence of foot/ground contact and friction.

Figure 7 illustrates the experimental setup used in this section. A six-axis load cell is used to measure the inertial forces and moments generated by the tail motions, which are then mapped into the equivalent forces and moments at the tail frame origin on the virtual quadruped robot using a Simulink-ADAMS co-simulation.

### B. Maneuvering Case Studies

The quadruped produced a 0.45 sec jump, as described in section II.A during which the tail, starting from a straight home configuration, produced planar tail motions to a final segment configuration while maintaining a fixed roll angle to enable rotation of the robotic system about the *z*-axis (Fig. 1). To measure the repeatability of these experiments and identify variability due to foot and ground impacts or

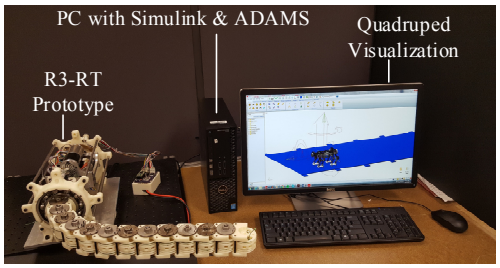

Fig. 7 Hardware-in-the-loop experimental setup.

friction upon landing, 5 trials were produced to achieve a desired set point $\theta_d = \{20, 10, 5\}°$ where the tail input angles were varied between $\beta_{seg,1,2} = -\{0{:}106,\ 0{:}52,\ 0{:}26\}°$, respectively. Results of the legged robot yaw angle $\theta$ from the simulated controller and HIL experimentally measured values are shown in Fig. 8. The RMS errors between steady state simulation and experimentally measured $\theta$ values at 0.8 sec are reported in Table II. The maximum quadruped turning the tail can produce without reaching its workspace limit of $\beta_{seg,1,2} = 120°$ was $\theta_d = 20°$. For this scenario, the tail produced the largest angular displacement. At the final tail configuration, static gravitational loading along the *z*-axis induced the greatest pitch and roll angular variation of the robot equivalent to 16° and 18.3° prior to ground impact of the rear, right leg – considered to be destabilizing effects due to maneuvering. The unbalanced orientation of the legged robot upon impact with the ground produces unbalanced forces that cause un-modeled rotational effects and deviation from the angular momentum conservation assumption, resulting in the largest RMS error of 5.14°. For the remaining case scenarios $\theta_d$ = 10° and 5°, since the tail produced motions with less angular displacements, the legged robot angular roll and pitch variation during the airborne phase is decreased due to less unbalanced gravitational loading effects which result in the quadruped landing in a more symmetric configuration; thus, reducing the undesirable effects of ground impact. It is for this reason the RMS error decreases with a reduction of $\theta_d$.

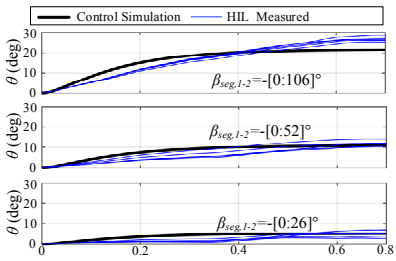

Fig. 8 Maneuvering control simulation and measured hardware-in-the-loop experiments for yaw angle turning of set points $\theta_d = \{20,10,5\}°$.

TABLE II. DESIRED SETPOINT TURNING ANGLE AND RMS ERROR

| Desired angle $\theta_d$ | RMS Error |
|---|---|
| 20° | 5.14° |
| 10° | 0.47° |
| 5° | -0.36° |

## VIII. CONCLUSION

This paper presented a dynamic modeling of a quadruped robot with an attached articulated tail. Dynamic formulations are used to select optimal ranges of tail mass and length ratio to produce more effective angular variation of the legged robot. Data on biological specimens was found to satisfy the optimal ranges defined based on analysis. The dynamic formulations were then used to derive an outer loop controller to plan tail trajectories for goal oriented behavior, and an inner loop controller was implemented by decoupling manipulator dynamics and controlling the tail to track a desired trajectory. The control approach performance was evaluated using hardware-in-the-loop simulations to demonstrate maneuvering case scenarios.

Future work will investigate articulated tail motion in combination with tail roll motion to reduce the effects of undesirable pitch and yaw motions of the legged robot during maneuvering applications for a smoother landing to minimize the yaw angle RMS error of the legged robot.

## REFERENCES


[1] R. Briggs, J. Lee, M. Haberland, and S. Kim, "Tails in Biomimetic Design: Analysis, Simulation, and Experiment," in *IEEE/RSJ International Conference on Intelligent Robots and Systems* Vilamoura-Algarve, Portugal, 2012, pp. 1473-1480, Vilamoura-Algarve, Portugal: IEEE, 2012.

[2] G. B. Gillis, L. A. Bonvini, D. J. Irschick, "Losing stability: tail loss and jumping in the arboreal lizard Anolis carolinensis," *J. of Experimental Biology,* vol. 212, no. 5, pp. 604-609, 2009.

[3] A. Jusufi, D. T. Kawano, T. Libby, and R. J. Full, "Righting and turning in mid-air using appendage inertia: reptile tails, analytical models and bio-inspired robots," *Bioinspiration & biomimetics,* vol. 5, no. 4, p. 045001, 2010.

[4] R. M. Brown, D. H. Taylor, and D. H. Gist, "Effect of caudal autotomy on locomotor performance of wall lizards (Podarcis muralis)," *Journal of Herpetology,* pp. 98-105, 1995.

[5] T. R. Kane and M. P. Scher, "A dynamical explanation of the falling cat phenomenon," *International Journal of Solids and Structures,* vol. 5, no. 7, pp. 663-670, 1969.

[6] S. Kajita and B. Espiau, "Legged robots," in *Springer handbook of robotics*: Springer, 2008, pp. 361-389.

[7] W. Saab and P. Ben-Tzvi, "Maneuverability and Heading Control of a Quadruped Robot Utilizing Tail Dynamics," in *Dynamic Systems and Control Conference*, VA, USA, 2017: ASME.

[8] W. Saab, W. Rone, and P. Ben-Tzvi, "Robotic Tails: A State of The Art Review," *Robotica (submitted July 2017, accepted,* 2018.

[9] F. J. Berenguer and F. M. Monasterio-Huelin, "Zappa, a quasi-passive biped walking robot with a tail: Modeling, behavior, and kinematic estimation using accelerometers," *IEEE Transactions on Industrial Electronics,* vol. 55, no. 9, pp. 3281-3289, 2008.

[10] A. Patel. M. Braae, "Rapid Acceleration and Braking: Inspirations From the Cheetah's Tail," in *International Conference on Robotics and Automation* Hong Kong, China, 2014, pp. 793-799.

[11] A. Patel and M. Braae, "Rapid Turning at High-Speed: Inspirations from the Cheetah's Tail," in *IEEE/RSJ International Conference on Intelligent Robots and Systems*, 2013, pp. 5506-5511: IEEE.

[12] E. Chang-Siu, T. Libby, M. Brown, R. J. Full, and M. Tomizuka, "A Nonlinear Feedback Controller for Aerial Self-Righting by a Tailed Robot," in *International Conference on Robotics and Automation* 2013, pp. 32-39: IEEE.

[13] A. Mutka, M. Orsag, and Z. Kovacic, "Stabilizing a Quadruped Robot Locomotion using a Two Degree of Freedom Tail," in *21st Mediterranean Conference on Control & Automation*, 2013, pp. 1336-1342.

[14] W. Rone and P. Ben-Tzvi, "Dynamic Modeling and Simulation of a Yaw-Angle Quadruped Maneuvering With a Planar Robotic Tail," *Journal of Dynamic Systems, Measurement, and Control,* vol. 138, no. 8, p. 084502, 2016.

[15] W. Saab, W. Rone, A. Kumar, and P. Ben-Tzvi, "Design and Integration of a Novel Spatial Articulated Robotic Tail," *Transactions on Mechatronics (accepted, pending revisions),* 2018.

[16] I. S. Godage, D. T. Branson, E. Guglielmino, G. A. Medrano-Cerda, and D. G. Caldwell, "Dynamics for biomimetic continuum arms: A modal approach," pp. 104-109: IEEE.

[17] M. W. Hannan and I. D. Walker, "Kinematics and the implementation of an elephant's trunk manipulator and other continuum style robots," *Journal of field robotics,* vol. 20, no. 2, pp. 45-63, 2003.

[18] T. Li, K. Nakajima, and R. Pfeifer, "Online learning for behavior switching in a soft robotic arm," pp. 1296-1302: IEEE.

[19] D. Braganza, D. M. Dawson, I. D. Walker, and N. Nath, "A neural network controller for continuum robots," *IEEE transactions on robotics,* vol. 23, no. 6, pp. 1270-1277, 2007.

[20] V. K. Chitrakaran, A. Behal, D. M. Dawson, and I. D. Walker, "Setpoint regulation of continuum robots using a fixed camera," *Robotica,* vol. 25, no. 5, pp. 581-586, 2007.

[21] D. B. Camarillo, C. R. Carlson, and J. K. Salisbury, "Configuration tracking for continuum manipulators with coupled tendon drive," *IEEE Transactions on Robotics,* vol. 25, no. 4, pp. 798-808, 2009.

[22] A. Bajo, R. E. Goldman, and N. Simaan, "Configuration and joint feedback for enhanced performance of multi-segment continuum robots," pp. 2905-2912: IEEE.

[23] I. A. Gravagne, C. D. Rahn, and I. D. Walker, "Large deflection dynamics and control for planar continuum robots," *IEEE/ASME transactions on mechatronics,* vol. 8, no. 2, pp. 299-307, 2003.

[24] W. Saab and P. Ben-Tzvi, "Design and Analysis of a Discrete Modular Serpentine Tail " in *International Design Engineering Technical Conferences & Computers and Information in Engineering Conference*, Charlotte, NC, USA, 2016, vol. Volume 5A, p. 8, Charlotte, NC, USA: ASME, 2016.

[25] W. Saab, W. Rone, and P. Ben-Tzvi, "Robotic Modular Leg: Design, Analysis and Experimentation," *Journal of Mechanisms and Robotics,* vol. 9, no. 2, 2016.

[26] W. S. Rone and T. Pinhas Ben, "Maneuvering and stabilizing control of a quadrupedal robot using a serpentine robotic tail," in *2017 IEEE Conference on Control Technology and Applications (CCTA)*, 2017, pp. 1763-1768.

[27] T. R. Kane and M. P. Scher, "Human self-rotation by means of limb movements," *J. of biomechanics,* vol. 3, no. 1, pp. 39-49, 1970.

[28] E. C.-Y. Yang, P. C. P. Chao, C.-K. Sung, "Optimal control of an under-actuated system for landing with desired postures," *IEEE Trans. on Control Sys. Tech.,* vol. 19, no. 2, pp. 248-255, 2011.

[29] T. Libby, A. M. Johnson, E. Chang-Siu, R. J. Full, and D. E. Koditschek, "Comparative design, scaling, and control of appendages for inertial reorientation," *IEEE Transactions on Robotics,* vol. 32, no. 6, pp. 1380-1398, 2016.

[30] A. Patel, E. Boje, C. Fisher, L. Louis, and E. Lane, "Quasi-steady state aerodynamics of the cheetah tail," *Biology Open,* 2016.

[31] A. Patel, "Understanding the motions of the cheetah tail using robotics," thesis 2015.

[32] P. E. Hudson, "The structural and functional specialisation of locomotion in the cheetah (Acinonyx Jubatus)," thesis 2011.